Available online at www.sciencedirect.com

ScienceDirect

Physics Procedia 56 (2014) 1277 – 1285

Physics Procedia

8th International Conference on Photonic Technologies LANE 2014

Neutron strain scanning of fibre and diode laser welds in stainless steel and Ti6Al4V

K.T. Voisey[a,*], J. Folkes[b], J. Srithorn[c], D.J. Hughes[d]

[a]*Faculty of Engineering, University of Nottingham, Nottingham, NG7 2RD, UK.*
[b]*Faculty of Engineering, University of Nottingham, Nottingham, NG7 2RD, UK (deceased).*
[c]*School of Industrial Engineering, Suranaree University of Technology, Thailand.*
[d]*WMG, University of Warwick, Coventry, CV4 7AL, UK.*

Abstract

Fibre lasers provide an unprecedented combination of high beam quality, brightness and low cost. Fibre laser beams can provide an exceptionally high power density beam with a relatively large depth of focus. Compared to more established laser welding technologies such as diode laser welding, fibre laser welding produces exceptionally narrow weld beads. As with all types of welding, fibre laser welding produces residual stresses in the material forming and adjacent to the weld. The SALSA instrument at the Institut Laue Langevin (ILL) has been used to make neutron diffraction measurements for both fibre and diode laser welded stainless steel 304 and Ti6Al4V. Clear diffraction peaks are obtained from stainless steel 304 and residual stress distributions are obtained. Little variation in residual stress distribution with welding parameters is seen. Ti6Al4V diffraction peaks are complicated by phase transformations on cooling. Transformed beta phase peaks in Ti6Al4V allow the extent of the heat affected zone to be determined.

Peer-review under responsibility of the Bayerisches Laserzentrum GmbH

Keywords: fibre laser; laser welding; residual stress; neutron diffraction

1. Introduction

The large power densities produced by focussed laser beams permit keyhole welding which produces higher aspect ratio welds than conduction welding (Matsunawa, Kim et al. 1998). This is advantageous since the total

* Corresponding author. Tel.: +44-115-951-4139 .
E-mail address: katy.voisey@nottingham.ac.uk

Peer-review under responsibility of the Bayerisches Laserzentrum GmbH
doi:10.1016/j.phpro.2014.08.051

energy input for a given weld depth is decreased, decreasing the extent of all the undesirable side effects of welding such as heat affected zones, distortion and residual stresses (Matsunawa, Kim et al. 1998). There is therefore significant industrial interest in laser welding and it has applications in the automotive and aerospace industries amongst others (Schubert, Klassen et al. 2001, Blackburn 2012).

Many different types of lasers can be used for welding. Fibre lasers are capable of producing an exceptionally high power density beam with a relatively large depth of focus, making them ideal for producing narrow, high aspect ratio welds (Quintino, Costa et al. 2007). Diode lasers have been successfully used in welding, where their robustness and efficiency makes them a suitable choice (Nasim and Jamil 2014).

As with all forms of welding, laser welding generates residual stresses. Knowledge of the residual stress distribution is vital to understand how the welded material will perform (Withers 2007), with fatigue and corrosion resistance (Dayal, Shaikh et al. 2008) of welds frequently being significantly worse than the parent material. Accurately predicting and controlling the residual stresses generated during welding is a challenging problem, hence the need for experimental measurements.

Residual stress distributions can be determined by a variety of means. The hole drilling and layer removal techniques are relatively simple but destructive methods. Whereas X-ray diffraction and neutron diffraction are non-destructive methods, with neutron diffraction having the advantage of being able to make measurements from sites several centimeters below the surface of metallic samples (Pardowska, Price et al. 2008). In neutron diffraction the lattice strain produced by residual stresses causes shifts in the position of the Bragg diffraction peaks. Measuring the peak shift as a function of location of the gauge volume allows the residual strain distribution to be determined, from which the residual stress distribution can be calculated. Minimum neutron diffraction gauge volumes are typically $1.5 \times 1.5 \times 2.0$ mm^3(Paradowska, Suder et al. 2010).

Paradowska et al.(Paradowska, Suder et al. 2010) have successfully used neutron diffraction to determine residual stress distributions for fibre laser welds in mild steel. Despite the weld width being approximately the same as that of the gauge volume for neutron diffraction, the use of small displacements of the gauge volume through the weld zone generated residual stress profiles with a spatial resolution of approximately 1.5 mm. Kumar et al. (Kumar, Kundu et al. 2013) have used neutron diffraction to determine the residual stress distribution in CO_2 laser welded P91 steel. Kabra et al. (Kabra, Brown et al. 2012) found good agreement between neutron diffraction measurements and predictions from modelling of laser welded titanium.

This work uses neutron strain scanning to determine the residual stresses generated by fibre and diode laser welding of stainless steel 304 and Ti6Al4V.

2. Experimental methods

2.1. Laser welding

Fibre and diode laser welded samples of stainless steel 304 (SS304) and Ti6Al4V were examined in this work. The welded samples were 50 x 50 x 1 mm in size, consisting of two 25 x 50 x 1mm pieces of material butt welded along the 50 mm edge. Each welded sample joined two pieces of the same material, i.e. SS304-SS304 and Ti6Al4V-Ti6Al4V welds were made. All welds were autogenous. Fibre laser welding was done using an IPG YLR 2000 fibre laser with 1.06 μm wavelength and maximum power of 2 kW. A ROFIN-SINAR DL 025 high power diode laser was used for the diode laser welds. In both cases the laser was focussed on the top surface of the samples. The diode laser was directly applied to the sample surface, i.e. no delivery fibre was used. During welding samples were clamped in position on an x-y table which was then translated under the laser head to generate the weld. Welding was carried out within a protective argon atmosphere.

For each type of laser, samples of each material were laser welded at a range of powers, 800-1600 W. The welding velocity varied with power, 300 to 800 mm/min for the diode laser and 3000 to 5000 mm/min for the fibre laser. As can be seen in Table 1 the energy input per unit length was significantly higher for the diode laser compared to the fibre laser. The power-velocity pairings used were the same for both materials and are detailed in Table 1, having been selected to give sound welds in previous work (Iammi 2009). It can be seen that the energy input per unit length of weld is significantly larger for the diode laser compared to the fibre laser, making diode laser welding a comparatively high energy input process compared to fibre laser welding.

Two additional fibre laser welds in SS304 at 1800 W and 900 W were used for preliminary carried out to demonstrate that SALSA was capable of determining the residual stress distributions in fibre laser welds.

Table 1. Power-velocity pairings.

Power (W)	Diode laser velocity (mm/min)	Diode laser energy per unit length (J/m)	Fibre laser velocity (mm/min)	Fibre laser energy per unit length (J/m)
800	300	160	3000	16.0
1000	400	150	3500	17.1
1200	500	144	4000	18.0
1400	700	120	4500	18.7
1600	800	120	5000	19.2

2.2. Neutron strain scanning

Neutron strain scanning was carried out using the SALSA instrument at the Institut Laue Langevin (ILL), Grenoble (experiment 1-01-74). The samples were mounted on a hexapod table and scanned through the incident neutron beam, a wavelength of 1.7 Å was used throughout this work. For the SS304 measurements the (311) austenite peak at 103º 2θ was used, for the Ti6Al4V the (101) alpha peak at 43º 2θ was used. For measurement of the transverse strain component in the SS304 samples the nominal gauge volume (the theoretical volume described by the beam optics) was 0.75 x 0.75 x 5 mm^3, with the 5 mm dimension parallel to the weld line and a count time of 2 minutes per point. For measurement of the longitudinal strain component in the SS304 samples a 0.75 x 0.75 x 0.9 mm nominal gauge volume was used, with the 1 mm dimension perpendicular to the weld lineDue to the smaller gauge volume, the count time was increased to 6 minutes per point. Thus, allowing for beam divergence, the sampled volume along the direction of interest was approximately 1 mm for all measurements. The measurement obtained was therefore an average of the strain state in the sampled volume of the material. In a steeply varying strain field this can lead to underestimation of the peak stresses. However, from the strain variations shown in figure 4, the choice of a 1 mm sampling volume is appropriate given the measured strain gradients.

For each sample the region from -10 mm to +20 mm, relative to the centreline of the weld was scanned. From -10 mm to +10 mm a measurement was made every 0.75 mm, between +10 mm and +20 mm the increment between successive measurement positions was increased to 1mm. A reference peak position corresponding to zero strain was found by obtaining a far field peak position from material at least 20 mm from the weld centreline. Raw data from SALSA was manipulated using the LAMP data handling programme, a dedicated piece of software produced by ILL (Richard, Ferrand et al. 1996). Strain was determined by measuring the 2θ shift of a selected diffraction peak for each material. Residual stresses were then calculated from the longitudinal and transverse strain results, using Young's modulus values of 193 GPa and 114 GPa for SS304 and Ti6Al4V respectively.

3. Results and discussion

Weld widths on SS304 ranged from 0.7 to 0.9 mm for the fibre laser welds and 2.4 to 2.9 mm for the diode laser welds (Fig. 1). For the Ti6Al4V weld widths ranged from 1.1 to 1.3 mm for the fibre laser and 3.8 to 4.3 mm for the diode laser (Fig. 2).

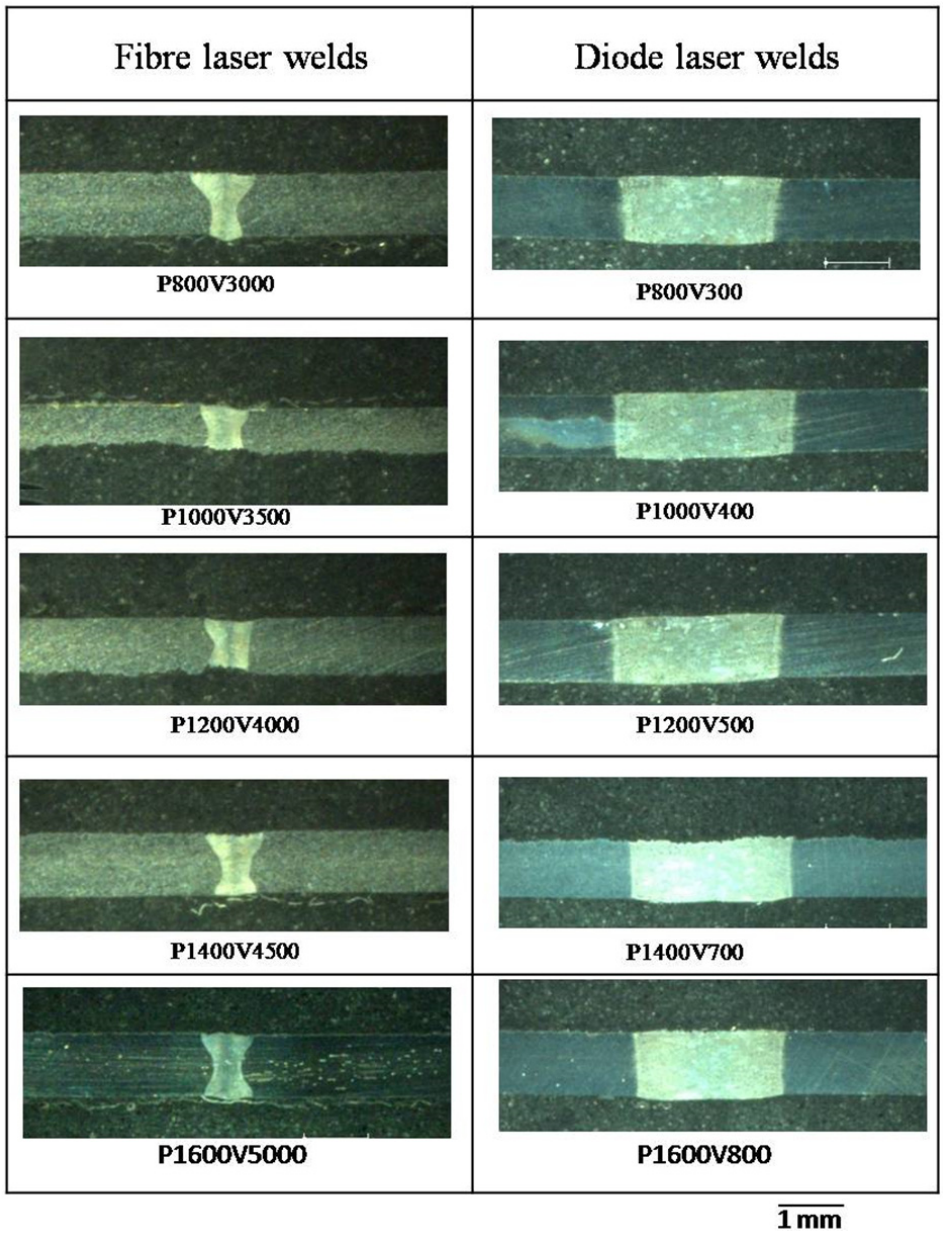

Fig. 1. Etched cross-sections of the fibre and diode laser welds in SS304.

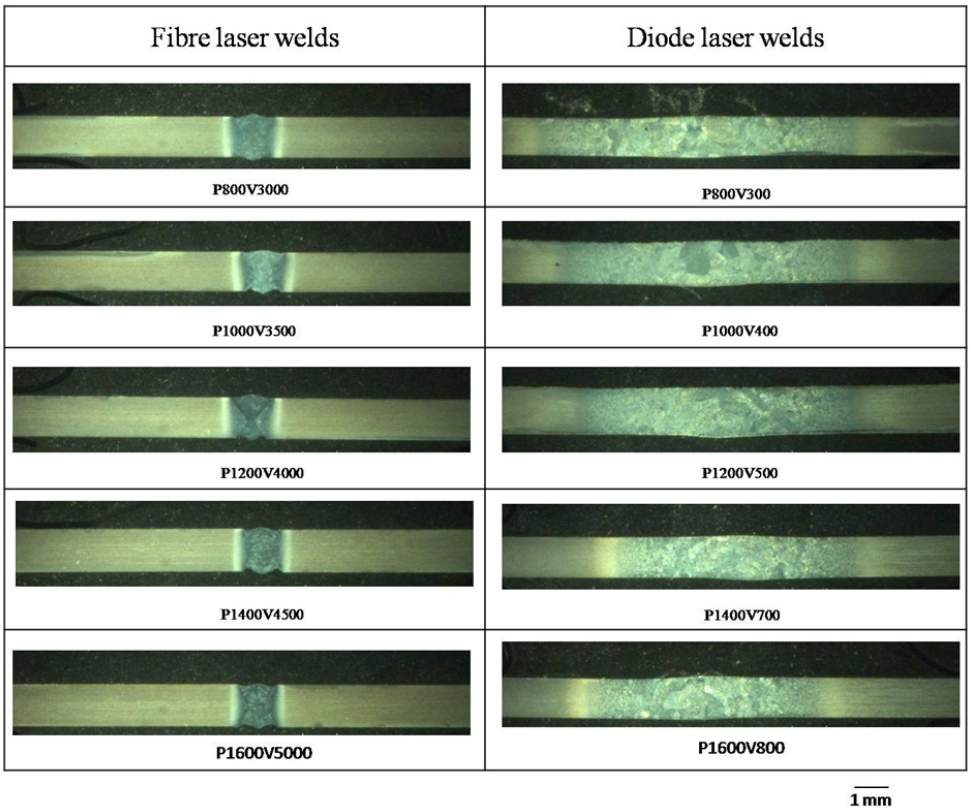

Fig. 2. Etched cross-sections of the fibre and diode laser welds in Ti6Al4V.

The preliminary results from the 1800 W and 900 W fibre laser welds in SS304 are shown in Fig. 3. The SS304 samples diffracted well, with clear peaks detected for each sample. The transverse and longitudinal components of stress are shown separately. For both power levels the transverse stress component is notably lower than the longitudinal component, as is typical in welds (Kou 2002). Therefore only the longitudinal stress component has been considered for the full set of samples. It should be noted that this preliminary work was done on samples with a different geometry to the rest of the welds considered, so the numerical values of the calculated stresses cannot be directly compared to the main set of experimental results.

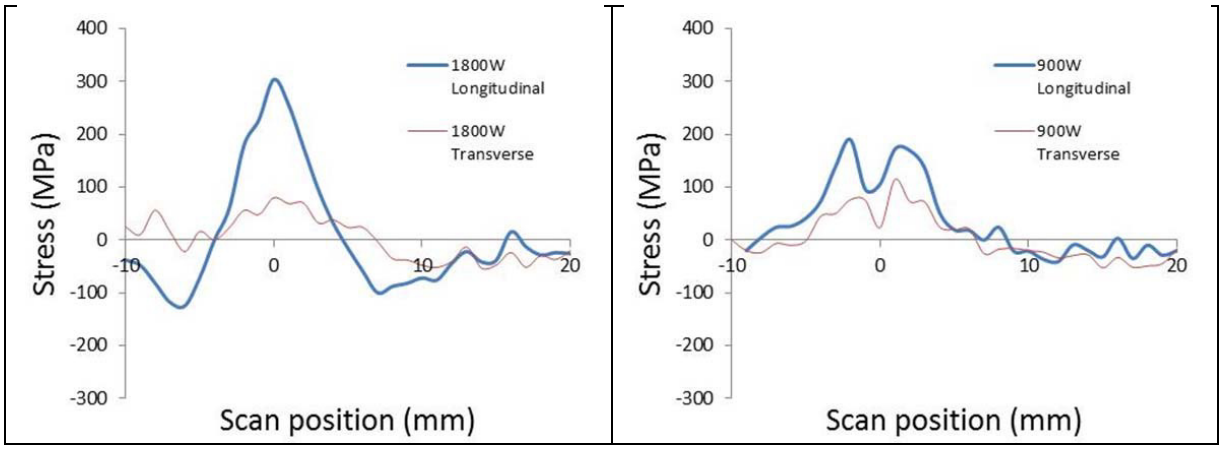

Fig. 3. Longitudinal and transverse residual stresses in 1800W and 900W SS304 fibre laser welds.

Figure 4 shows the longitudinal and transverse residual strain measurements for diode and fibre laser welded SS304. The resulting, dominant, longitudinal component of residual stress is also shown for all SS304 welds in Fig. 4. For both fibre and diode laser welds all residual stress distributions are typical of those expected in welding (Kou 2002), with a tensile region in the weld bead and a balancing compressive stress region in the surrounding material. The width of the tensile regions of the stress distributions is consistent with the width of the weld beads, with that of the fibre laser welded samples being markedly narrower than that of the diode laser welds. This is consistent with the wider weld area and increased heat input in the diode laser welding process. Although the full extent of the compressive region of the diode laser welds cannot be seen it is clear that this is approximately the same for both types of welding even though the weld beads are of different sizes. For both sets of results the centre of symmetry of the stress distribution is off-set with respect to the zero on the x-axis. This is simply an artefact resulting from the sample alignment process. The stress distributions are, as expected, symmetrical about the real centreline of the weld.

For both types of laser welding, there is little variation in residual stress distribution as a function of laser power. There is little difference in the magnitude of the tensile peak between the diode and fibre laser welding processes and the peak is, as expected, similar to the yield strength of 304SS (290 MPa). This result is also in agreement with results observed for DC GMAW (Gas Metal Arc Welding), pulsed GMAW, hybrid laser and autogenous laser welds of 4 mm ASTM A131 steel; grade DH36 (Colegrove P., Ikeagu C. et al. 2009), yield strength 355 MPa, where very little difference in the magnitude of the tensile peak was observed between the different welding processes.

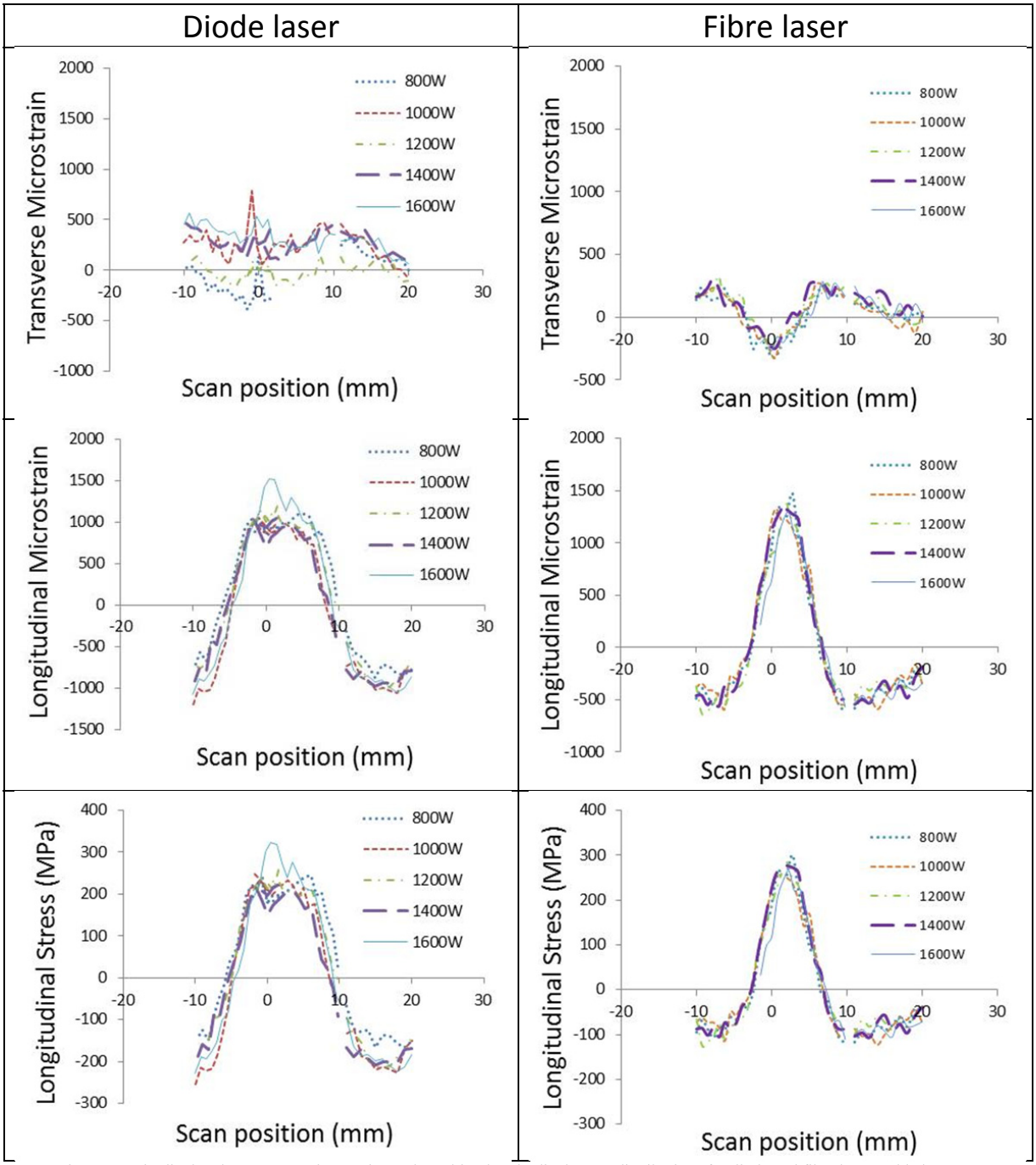

Fig. 4. Longitudinal and transverse microstrains and resulting longitudinal stress distributions for diode and fibre laser welded SS304.

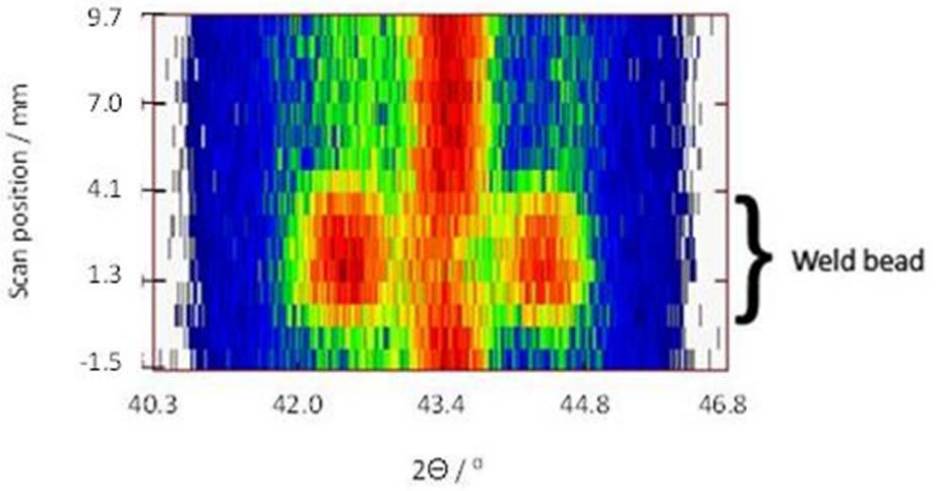

Fig. 5. Measured diffracted intensity as a function of 2θ for Ti6Al4V with a 800W fibre laser weld.

Ti6Al4V is an alpha/beta alloy. The Ti6Al4V welds are surrounded by a heat affected zone, containing significantly more transformed beta phase than in the non-affected material. The main diffraction peak measured for Ti6Al4V was the alpha (101) peak. As for the SS304 results, the variation in position of this peak can theoretically be used to determine the residual stress distribution. However, during the course of the neutron measurements it was found that the welded Ti6Al4V plates were highly textured. This resulted in the amplitude of the diffraction peak varying significantly with the relative orientation of the texture direction and the incident neutron beam and made it impossible to reliably determine the residual stress distribution.

Nevertheless, as can be seen in Fig. 5, as well as the shift of the main (101) peak, additional peaks appear in some of the scans. These additional peaks are attributed to the transformed beta phase that occurs in the weld bead and heat affected zone. This means that analysis of the Ti6Al4V can be used to indicate the location of the weld and the extent of the heat affected zone.

4. Summary and conclusions

SALSA has been used for strain measurement of fibre and diode laser welded SS304 and Ti6Al4V. SS304 diffracted well, producing results that were straightforward to process. Residual stress distributions have been determined for the SS304 samples. Classic weld residual stress distributions with high tensile stresses in the weld bead and immediately adjacent material surrounded by relatively wide regions of low tensile stresses were seen in each sample. A clear difference in width of the distribution is seen between the fibre and diode laser welds. This correlates with the observed difference in width of the welds and is consistent with the difference in energy input per unit length of the two processes, with wider welds being produced by the higher energy per unit length diode welding process. No clear trend between the stress distributions and laser power is seen for either set of samples. However, it should be noted that final residual stress distributions will have been modified by sample distortion occurring after welding, the material on either side of the weld is not co-planar, rotations of up to 1.2º about the weld line have been measured.

The Ti6Al4V diffraction results were complicated by a high degree of texture in the welded material. This was transverse to the welding direction. The appearance of additional peaks is attributed to the presence of the transformed beta phase in the weld bead and heat affected zone. Analysis of the Ti6Al4V results has the potential to indicate the presence or absence of the alpha and transformed beta phases at each scan position, thereby revealing

the extent of the heat affected zone, as well as determining the residual stress distribution. Of course metallographic sectioning is a markedly simpler and cheaper, albeit destructive method that could reveal the heat affected zone. The use of neutron strain scanning for this purpose is hard to justify and would practically be restricted to particularly high value components where destructive testing is simply not an option or for research work, the results of which would feedback into practical applications.

References

LAMP, the Large Array Manipulation Program. http://www.ill.fr/data_treat/lamp/lamp.html

Blackburn, J. (2012). Laser welding of metals for aerospace and other applications. Cambridge, Woodhead Publ Ltd.

Colegrove P., Ikeagu C., Thistlethwaite A., Williams S., Nagy T., Suder W., Steuwer A. and Pirling T. (2009). "Welding process impact on residual stress and distortion." Science and Technology of Welding and Joining **14**: 717-725.

Dayal, R. K., H. Shaikh and N. Parvathavarthini (2008). Corrosion issues in ferrous weldments. Cambridge, Woodhead Publ Ltd.

Iammi, J. (2009). Fibre laser welding of AISI 304 and Ti-6Al-4V. PhD, University of Nottingham.

Kabra, S., D. W. Brown, C. F. Chen, T. K. Wong and J. O. Milewski (2012). "MEASUREMENT AND SIMULATION OF RESIDUAL STRAIN IN A LASER WELDED TITANIUM RING." Welding in the World **56**(1-2): 2-8.

Kou, S. (2002). Welding Metallurgy, John Wiley & Sons.

Kumar, S., A. Kundu, K. A. Venkata, A. Evans, C. E. Truman, J. A. Francis, K. Bhanumurthy, P. J. Bouchard and G. K. Dey (2013). "Residual stresses in laser welded ASTM A387 Grade 91 steel plates." Materials Science and Engineering a-Structural Materials Properties Microstructure and Processing **575**: 160-168.

Matsunawa, A., J. D. Kim, N. Seto, M. Mizutani and S. Katayama (1998). "Dynamics of keyhole and molten pool in laser welding." Journal of Laser Applications **10**(6): 247-254.

Nasim, H. and Y. Jamil (2014). "Diode lasers: From laboratory to industry." Optics & Laser Technology **56**(0): 211-222.

Paradowska, A. M., W. Suder and S. Williams (2010). "Neutron Diffraction Residual Stress Measurements in Key-Hole Laser Formed Weldments." International Conference on Neutron Scattering 2009 **251**.

Pardowska, A. M., J. W. H. Price, R. Ibrahim and T. R. Finlayson (2008). "Neutron diffraction evaluation of residual stress for several welding arrangements and comparison with fitness-for-purpose assessments." Journal of Pressure Vessel Technology-Transactions of the Asme **130**(1).

Quintino, L., A. Costa, R. Miranda, D. Yapp, V. Kumar and C. J. Kong (2007). "Welding with high power fiber lasers - A preliminary study." Materials & Design **28**(4): 1231-1237.

Richard, D., M. Ferrand and G. J. Kearley (1996). "Analysis and Visualisation of Neutron-Scattering Data " J. Neutron Research **4**: 33-39.

Schubert, E., M. Klassen, I. Zerner, C. Walz and G. Sepold (2001). "Light-weight structures produced by laser beam joining for future applications in automobile and aerospace industry." Journal of Materials Processing Technology **115**(1): 2-8.

Withers, P. J. (2007). "Residual stress and its role in failure." Reports on Progress in Physics **70**(12): 2211-2264.